Breast Cancer Res Treat (2016) 160:523–530
DOI 10.1007/s10549-016-4022-6

EPIDEMIOLOGY

Internal mammary node adenopathy on breast MRI and PET/CT for initial staging in patients with operable breast cancer: prevalence and associated factors

Hyejin Cheon[1] · Hye Jung Kim[1] · Sang-Woo Lee[2] · Do-Hoon Kim[2] · Chang-Hee Lee[2] · Seung Hyun Cho[1] · Kyung Min Shin[1] · So Mi Lee[1] · Gab Chul Kim[1] · Won Hwa Kim[1]

Received: 12 October 2016 / Accepted: 13 October 2016 / Published online: 17 October 2016

Abstract
Purpose To evaluate the prevalence of and factors associated with internal mammary node (IMN) adenopathy on MRI and PET/CT used for initial staging in patients with operable breast cancer.
Methods A total of 1320 patients diagnosed with invasive breast carcinoma between January 2011 and December 2015 underwent MRI and PET/CT for initial staging. The patients were considered to have IMN adenopathy when MRI revealed IMNs with the longest diameter of 5 mm or greater and a standardized uptake value greater than that of the mediastinal blood pool/contralateral parasternal area on PET/CT. The prevalence was determined as overall percentage of patients with IMN adenopathy, as well as percentages among patients who received neoadjuvant chemotherapy and those who did not. The association of IMN adenopathy with factors was evaluated using multivariate logistic regression analysis.
Results Of the 1320 patients, 35 patients [2.7 %; 95 % confidence interval (CI) 1.8–3.6 %] had IMN adenopathy, with a total of 49 IMNs. Among patients without and with neoadjuvant chemotherapy ($n = 1092$ and $n = 228$, respectively), IMN adenopathy was identified in 13 (1.2 %; 95 % CI 0.6–2.0 %) and 22 patients (9.6 %; 95 % CI 6.0–14.6 %), respectively. Inner tumor location [odds ratio (OR) 5.9; $P = .002$] and positive axillary lymph node status (OR 4.4; $P < .0001$) were associated with IMN adenopathy.
Conclusions IMN adenopathy was identified at initial staging with PET/CT and MRI with a prevalence of 2.7 %. Inner tumor location and positive axillary lymph node status were associated with IMN adenopathy.

Keywords Invasive breast cancer · Breast MRI · PET–CT · Internal mammary node · IMN adenopathy

Introduction

In breast cancers, patients with internal mammary node (IMN) adenopathy have a worse prognosis than those without IMN adenopathy, as recognized by the 7th edition of the American Joint Committee on Cancer staging criteria. The presence of clinically detected IMN metastases results in the upstaging of a patient to N2b in the absence of axillary lymph node metastases and to N3b in the presence of 1–9 axillary lymph node metastases [1]. Although the management of IMNs has long been debated, previous studies demonstrate that treatment of IMNs with radiation and/or adjuvant chemotherapy may improve clinical outcomes in patients with advanced-stage breast cancer [2, 3]. In addition, recent studies have shown that irradiation of IMNs improves survival in patients with early-stage breast cancer [4–6]. However, radiation therapy to IMNs may cause cardiac toxicity and increase the rate of major coronary events [7]. Therefore, the identification of IMN adenopathy prior to the initiation of treatment is important in the management of patients diagnosed with breast cancer.

The optimal tool for evaluating IMN adenopathy has not been established. Lymphoscintigraphy is one of the tools

✉ Won Hwa Kim
greenoaktree9@gmail.com

[1] Department of Radiology, Kyungpook National University Medical Center, 807 Hoguk-ro, Buk-gu, Daegu 41404, Korea

[2] Department of Nuclear Medicine, Kyungpook National University Medical Center, 807 Hoguk-ro, Daegu 41404, Korea

for the detection of IMN drainage; however, visualized IMN drainage does not signify nodal involvement [8]. Internal mammary sentinel lymph node biopsy followed by lymphoscintigraphy is the most definitive test to evaluate IMNs, but it is not a standardized practice, having variable success rates and a relatively high rate of complications, such as pleural breach and internal mammary vessel injury [9, 10]. Positron emission tomography/computed tomography (PET/CT) and breast magnetic resonance imaging (MRI) have been used for initial staging in patients diagnosed with breast cancer with regard to the primary tumor or axillary staging [11–14]. Extra-axillary lymph node metastasis, including metastasis to the IMNs, as well as distant metastasis, can also be evaluated using PET/CT [14, 15]. Breast MRI, considered the most accurate imaging modality for providing anatomical information about bilateral breasts, allows visualization of the parasternal area. To the best of our knowledge, few reports to date have focused on IMN evaluation at initial staging using breast MRI and PET/CT, and these have been limited to small populations or patients only with advanced-stage breast cancer [16, 17]. Assessment for the prevalence of and factors associated with IMN adenopathy using breast MRI and PET/CT in patients with operable breast cancer may provide information crucial for the cancer management.

Therefore, the purpose of the current study was to evaluate the prevalence of and factors associated with IMN adenopathy on breast MRI and PET/CT used for initial staging in patients with operable breast cancer.

Materials and methods

This study was approved by our institutional review board and the requirement for informed consent was waived.

Study population

From a review of the breast imaging database of Kyungpook National University Medical Center, we identified 1441 consecutive patients with invasive breast cancer who underwent both breast MRI and PET/CT before curative surgery between January 2011 and December 2015. At our institution, breast MRI and PET/CT have been routinely performed for initial staging in patients with biopsy-confirmed breast cancer. Among the 1441 initial patients, we excluded women with a past history of breast cancer ($n = 57$), excisional biopsy ($n = 50$) before breast MRI and PET/CT, and bilateral breast cancers ($n = 14$). The remaining 1320 patients were included in this study.

Image acquisition

Breast MRI was performed with the patient prone on a 3.0-T system (Discovery MR750, GE Healthcare) with a dedicated four- or eight-channel surface breast coil. Each patient received 0.1 mL/kg of gadobutrol IV (Gadovist, Bayer Schering Pharma, Berlin, Germany) as the contrast agent injected as a bolus at a rate of 1 mL/s. Axial T1-weighted (TR/TE, 699/10.5; matrix, 352 × 256; slice thickness, 3 mm); axial T2-weighted with fat saturation (TR/TE, 8353/90; matrix, 384 × 256; slice thickness, 3 mm); axial T1-weighted with dynamically contrast-enhanced fat saturation images (TR/TE, 4.2/1.2; matrix, 288 × 416; slice thickness, 2 mm); and subtracted and maximum intensity projection (MIP) images were also generated. The parasternal area was adequately visualized on all breast MRI examinations.

For PET/CT, whole-body scanning was performed on a PET/CT system with a Reveal RT-HiREZ 6-slice CT apparatus® (CTI Molecular Imaging, Knoxville, TN, USA) and 16-slice CT Discovery STE PET/CT apparatus®, 16-slice CT Discovery 600 apparatus®, or 64-slice CT Discovery 690 apparatus® (GE Healthcare, Milwaukee, WI, USA) after patients had fasted for at least 6 h. Approximately 3.7–5.55 MBq of [^{18}F]-fluorodeoxyglucose (FDG)/kg of body weight was injected intravenously (IV), and the patients were advised to rest for 1 h before image acquisition. For attenuation correction before the PET scan, a low-dose CT scan was obtained without contrast enhancement from the base of the skull vertex continuing to the knee with the patient in the supine position with quiet respiration. PET was performed with a maximum spatial resolution of 6.5 mm (Reveal PET/CT), 5.5 mm (Discovery PET/CT), 5.1 mm (Discovery 600 PET/CT), and 4.9 mm (Discovery 690 PET/CT) at 1.5 or 3 min per bed position.

Image analysis

Two breast imaging radiologists (H.J.C and W.H.K., with 5 and 10 years of experience, respectively) and two nuclear medicine physicians (D.H.K and S.W.L, with 5 and 19 years of experience, respectively) retrospectively reviewed the MRI and PET/CT images. Patients were considered to have IMN adenopathy when MRI revealed IMNs with the longest diameter of 5 mm or greater [16] and a standardized uptake value (SUV) greater than that of the mediastinal blood pool or parasternal area on PET/CT [17, 18]. The location, size (short- and long-axis measurements), L/S ratio (ratio of long- to short-axis diameter),

shape (oval or round), and presence of fatty hilum for each IMN were recorded.

The maximum SUV (SUVmax) of each IMN was calculated using the volume viewer software on a GE Advantage Workstation 4.3 (GE Healthcare) with the following formula:

$$\text{SUVmax} = \frac{\text{maximum activity in region of interest (MBq/g)}}{\text{injected dose (MBq)/body weight (g)}}$$

Method for confirmation

Histopathologic confirmation was not done to determine IMN metastasis. Decrease in either size or SUV of IMN after treatment in follow-up imaging including breast MRI ($n = 19$), PET/CT ($n = 21$), and chest CT ($n = 12$) with aforementioned imaging criteria was considered as IMN adenopathy for metastatic lymphadenopathy.

Data collection and statistical analysis

Clinical data collected included age at cancer diagnosis and status of neoadjuvant chemotherapy. The following histopathological information was included from surgical specimens and percutaneous biopsy results: histologic tumor characteristics; tumor grade; estrogen receptor (ER), progesterone receptor (PR), and human epidermal growth factor receptor (HER2) status; and axillary nodal status. The expression of ER, PR, and HER2 was assessed by immunohistochemical staining. Expression of ER and PR was quantified using the Allred score, considering a total Allred score >2 as positive for ER or PR [19]. A HER2 value of 0 or 1 was considered negative (HER2-negative) and a value of 3 was considered positive (HER2-positive). A HER2 value of 2 was considered equivocal; for equivocal cases, silver-enhanced in situ hybridization was performed and a HER2/CEP17 ratio ≥2.0 or a HER2/CEP17 ratio <2.0 with an average HER2 copy number ≥6.0 were considered positive (HER2-positive) [20]. Hormone receptor (HR) positive status was defined as tumors expressing ER and/or PR. The axillary lymph node status was determined by surgical results, but in the neoadjuvant chemotherapy group, the axillary lymph node status was determined by the pathological results of fine-needle aspiration or clinical nodal staging. Imaging findings of tumor size and location were recorded.

The prevalence with 95 % confidence intervals (CIs) was determined as the overall percentage of patients with IMN adenopathy and the percentages among patients who received neoadjuvant chemotherapy and those who did not. The clinicopathological and imaging findings of patients with and without IMN adenopathy were compared using the Chi square test or Fisher's exact test as appropriate. The odds ratio (OR) and 95 % CI for IMN adenopathy were calculated with univariate logistic regression analysis, and variables with $P < .10$ were selected for the final multivariate model. All statistical analyses were performed with statistical software (SPSS version 24.0 software; Chicago, IL, USA), and $P < .05$ was considered to indicate a statistically significant difference.

Table 1 Imaging characteristics of internal mammary node adenopathy on BREAST MRI and PET/CT in 35 patients with 49 internal mammary nodes

Variable	No. of internal mammary nodes (%)
Location	
First intercostal	20 (40.8)
Second intercostal	17 (34.7)
Third intercostal	7 (14.3)
Fourth intercostal	5 (10.2)
Size, long axis	
≤1 cm	28 (57.1)
1–1.5 cm	15 (30.6)
>1.5 cm	6 (12.2)
Size, short axis	
≤0.5 cm	20 (40.8)
0.5–1.0 cm	24 (49.0)
>1.0 cm	5 (10.2)
Shape	
Oval (L/S ≥1.5)	35 (71.4)
Round (L/S <1.5)	14 (28.6)
Fatty hilum	
Absent	49 (100.0)
Present	0 (0.0)
SUV	
1.5–2.0	14 (28.5)
2.0–4.0	19 (38.8)
>4.0	16 (32.7)

SUV standardized uptake value, *L/S* ratio of long- to short-axis diameter

Results

Study population

The median age of the 1320 patients was 49.0 years (range 25–83 years). The median tumor size was 2.4 cm (range

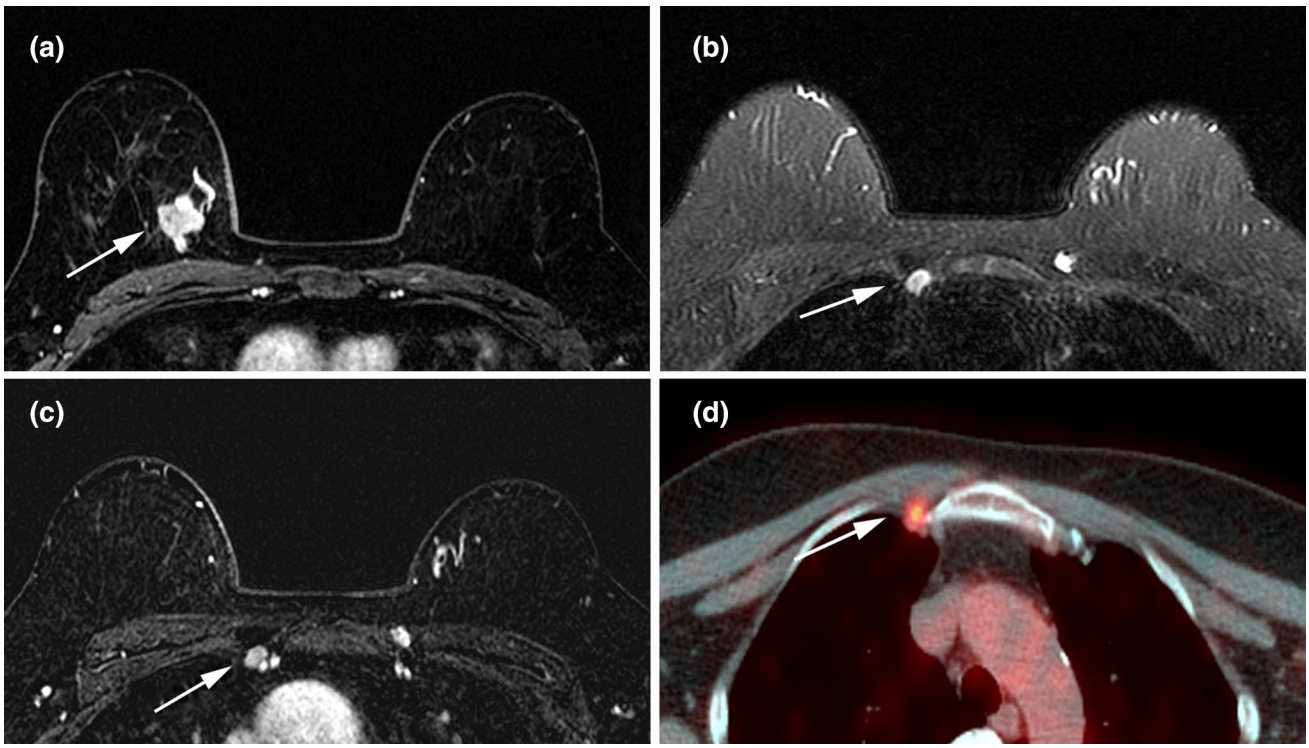

Fig. 1 Images of a 58-year-old woman with internal mammary adenopathy on both breast MRI and PET/CT examinations. **a** T1-weighted axial contrast-enhanced breast MR image shows a 2.4-cm mass (*arrow*) in the right inner breast. **b**, **c** T2-weighted axial breast MR image and T1-weighted axial contrast-enhanced breast MR image show an 11-mm internal mammary node (*arrow*) in the first intercostal space. **d** Axial PET/CT image reveals focal FDG uptake (*arrow*) in the same location with a maximum standardized uptake value of 4.1

0.4–12 cm). Of the 1320 patients, 228 patients (17.3 %) received neoadjuvant chemotherapy before curative surgery. Based on the tumor size at initial staging, 1086 patients (82.3 %) had tumors with the longest diameter ≤5 cm, and 234 patients (17.7 %) had tumors with the longest diameter >5 cm. Of the 228 patients who received neoadjuvant chemotherapy, 198 patients (86.8 %) had clinically positive axillary lymph nodes. Of the 1092 patients who did not receive neoadjuvant chemotherapy, 307 patients (28.1 %) had pathologically positive axillary lymph nodes.

Prevalence and characteristics of IMN adenopathy

On breast MRI and PET/CT, IMN adenopathy was identified in 35 patients (2.7 %; 95 % CI 1.8–3.6 %) with 49 IMNs; 24 patients (68.6 %) had one positive IMN, 7 patients (20.0 %) had two positive IMNs, 3 patients (8.6 %) had three, and 1 patient (2.9 %) had four. In patients without and with neoadjuvant chemotherapy, IMN adenopathy was identified in 13 patients (1.2 %; 95 % CI 0.6–2.0 %) and 22 patients (9.6 %; 95 % CI 6.0–14.6 %), respectively. The median SUVmax of 49 IMNs and 35 IMNs showing the maximum SUVmax per patient was 2.8 (range 1.5–13.7) and 3.2 (range 1.5–13.7). The detailed imaging characteristics of 49 IMNs are described in Table 1. The median size of the IMNs was 1.0 cm in the longest axis (range 0.6–2.1 cm) and 0.6 cm (range 0.3–1.4 cm) in the shortest axis. The median L/S ratio was 1.7 (range 1.0–3.5). All IMNs showed loss of fatty hilum. The first intercostal space was the most frequent location of IMN adenopathy ($n = 20$, 40.8 %) (Fig. 1).

Factors associated with IMN adenopathy

On univariate analysis, factors associated with IMN adenopathy were larger (>5 cm) tumor size ($P = .007$), tumor location ($P = .001$), and positive axillary lymph node status ($P < .0001$) (Table 2). On multivariate analysis, inner tumor location ($P = .002$) and positive axillary lymph node status ($P < .0001$) were independently associated with IMN adenopathy (Table 3).

Discussion

Although the incidence of IMN metastasis has been reported in old series of surgical IMN evaluation from extended mastectomy [21, 22], the detection of IMN

Table 2 Comparison of clinicopathologic and imaging findings between patients without and with internal mammary node adenopathy

Variable	Patients without IMN adenopathy ($n = 1285$)[a]	Patients with IMN adenopathy ($n = 35$)[a]	OR	95 % CI	*P* value
Age (years)					.494
<50	646 (50.3)	20 (57.1)	1.00		
≥50	639 (49.7)	15 (42.9)	0.76	0.39, 1.49	
Tumor size					.007
≦5 cm	1088 (84.7)	23 (65.7)	1.00		
>5 cm	197 (15.3)	12 (34.3)	2.88	1.41, 5.89	
Tumor location					.001
Outer	539 (41.9)	6 (17.1)	1.00		
Central	401 (31.2)	11 (31.4)	2.46	0.90, 6.72	
Inner	234 (18.2)	9 (25.7)	3.46	1.22, 9.82	
Multicentric	111 (8.6)	9 (25.7)	7.28	2.54, 20.88	
Histologic tumor characteristics		35			.789
Ductal, NOS	1172 (91.2)	33 (94.3)	1.00		
Lobular	44 (3.4)	1 (2.9)	0.81	0.11, 6.04	
Others[c]	69 (5.4)	1 (2.9)	0.52	0.07, 3.82	
Tumor grade[b]					.277
Low	182 (14.4)	2 (5.7)	1.00		
Intermediate	714 (56.5)	20 (57.1)	2.55	0.59, 11.01	
High	368 (29.1)	13 (37.1)	3.22	0.72, 14.40	
Hormonal receptor status					.116
Positive	959 (74.6)	22 (62.9)	1.00		
Negative	326 (25.4)	13 (37.1)	1.74	0.87, 3.49	
HER2 status					.062
Negative	982 (78.2)	22 (64.7)	1.00		
Positive	274 (21.8)	12 (35.3)	1.96	0.96, 4.00	
Axillary lymph nodal status					< .0001
Negative	805 (62.6)	10 (28.6)	1.00		
Positive	480 (37.4)	25 (71.4)	4.19	2.00, 8.81	

IMN internal mammary node, *CI* confidence interval, *OR* odds ratio, *HER2* human epidermal growth factor receptor 2, *NOS* not otherwise specified

[a] Data are numbers of patients, with percentages in parentheses

[b] Limited to patients ($n = 1299$) with available tumor grade results

[c] Others include mucinous (31), metaplastic (18), papillary (8), tubular (7), adenoid cystic (3), medullary (2), cribriform (1)

adenopathy by imaging, especially breast MRI, has rarely been investigated. In the present study, we evaluated IMN adenopathy detected by imaging with breast MRI and PET/CT at initial staging in a population of 1320 patients with breast cancer, and found the prevalence of IMN adenopathy to be 2.7 % overall, 1.2 and 9.6 % in groups without and with neoadjuvant chemotherapy. We also described the characteristics of IMN adenopathy on breast MRI showing significant FDG uptake on PET/CT; all IMNs were discretely observed on breast MRI with a median size of 1 cm and loss of fatty hilum.

Our study suggests that breast MRI, in spite of controversy regarding its generalized use as a preoperative staging modality, could be useful as an imaging tool to assess extra-axillary lymph node metastasis including the parasternal area [23–25]. Furthermore, breast MRI could be used to identify IMN adenopathy in early-stage breast cancer in which PET/CT may not routinely be performed for initial staging. Recently, there has been renewed interest in the elective irradiation of the regional lymph nodes including the IMNs and the medial supraclavicular lymph nodes due to its favorable effects and the improved techniques available for its delivery. The results of the European Organization for the Research and Treatment of Cancer 22922/10925 study showed improved disease-free survival and distant disease-free survival with irradiation of

Table 3 Multivariate analysis of factors associated with internal mammary node adenopathy

Variable	OR	95 % CI	*P* value
Tumor size			
≦5 cm	1.00		
>5 cm	1.65	0.52–5.29	.397
Tumor location			.019
Outer	1.00		
Central	2.90	0.99–8.51	.053
Inner	5.88	1.89–18.29	.002
Multicentric	3.83	0.92–15.86	.065
HER2 status			
Negative	1.00		
Positive	1.44	0.68–3.07	.345
Axillary lymph nodes status			
Negative	1.00		
Positive	4.35	1.93–9.79	< .0001

OR odds ratio, *CI* confidence interval; *HER2* human epidermal growth factor receptor 2

IMNs and medial supraclavicular lymph nodes [5]. In the Danish Breast Cancer Cooperative Group 82b and 82c trials, irradiation of IMNs also increased overall survival in patients with early-stage node-positive breast cancer [4]. Therefore, the careful identification of IMN adenopathy on breast MRI as well as PET/CT, with knowledge of its prevalence and associated factors, is increasingly important in order to provide patients with the opportunity to receive adjuvant therapy including radiotherapy and/or chemotherapy.

In our study, most of the patients had relatively small tumors (≤5 cm, 82.3 %) and did not undergo neoadjuvant chemotherapy (82.7 %). As a result, the overall prevalence of IMN adenopathy (2.7 %) was lower in our study than that observed in prior studies that focused on patients with advanced-stage breast cancer. In a prior study with PET/CT, the authors found that 9 % (110/1259) of patients had positive IMNs with unknown population characteristics regarding the primary tumor size or neoadjuvant chemotherapy [26]. Another study, involving patients with neoadjuvant chemotherapy, demonstrated a prevalence of IMN adenopathy of 16 % (14/90) on PET/CT and MRI; this was also higher than the rate of 10 % (22/228) observed in the group with neoadjuvant chemotherapy in the present study [17].

The current study also confirmed that inner tumor location and positive axillary lymph node status were independently associated with IMN adenopathy. These findings are largely consistent with those of previous studies, which have shown that the risk of IMN involvement is higher in patients with larger primary tumors, medial tumors, positive axillary nodes, and age younger than 50 years [2, 6, 27]. Among the risk factors, it is notable that inner tumor location was associated with the highest risk for IMN adenopathy (OR 5.9) in our results. This finding can be explained by the lymphatic drainage pattern of the breast, in which IMN drainage is significantly more common from quadrants other than the upper outer quadrant, although drainage to the IMN occurs in all quadrants [8]. However, in contrast to prior studies, independent association of IMN adenopathy with larger tumor size was not shown in our multivariate analysis, although there was a significant association in univariate analysis. In addition, younger age (<50 years) was not significantly associated with IMN adenopathy in our findings.

The major limitation of our study is that all IMNs were presumed pathologic according to a reference standard based on our imaging criteria and follow-up imaging without histopathologic confirmation. However, histopathologic confirmation of IMNs is not a standard practice in many institutions, and IMNs have more commonly been evaluated by imaging studies, particularly with PET/CT. Nonetheless, specific imaging criteria for IMN involvement have not been established. In previous studies using PET/CT, positive IMNs were determined visually [17, 26, 28]; the mean SUVmax ranged from 3.5 to 3.7, and the ranges of SUVmax varied from 0.9 to 20.3. In our study, the median SUVmax per patient was 3.2 and the ranges were 1.5–13.7. For breast MRI, according to a recent study involving screening for high-risk patients, non-malignant IMNs were visualized with an average size of 4–4.5 mm (range 2–10 mm) and a visible fatty hilum or a normally shaped lobular or oval appearance with circumscribed margins [29, 30]. In contrast, the size range of presumed metastatic IMNs in a previous study was 7–22 mm [17], and the range was 6–21 mm with a median size of 11 mm and loss of fatty hilum in all IMNs in the current study.

Our study has several other limitations. This was a retrospective study performed at a single institution. Although breast MRI and PET/CT for initial staging in consecutive patients newly diagnosed with breast cancer were routinely performed during this period, we did not control for a possible selection bias of patients who underwent breast MRI and PET/CT. In addition, this study did not evaluate the IMNs observed on breast MRI that did not show increased FDG uptake on PET/CT in patients with breast cancer, and further studies are warranted to explore the prevalence or prognostic value of IMNs seen on MRI not showing increased FDG uptake on PET/CT.

In conclusion, IMN adenopathy was identified at initial staging with PET/CT and MRI with a prevalence of 2.7 % in patients with operable breast cancer. Inner tumor

location and positive axillary lymph node status were independently associated with IMN adenopathy.

Acknowledgments This work was supported by Biomedical Research Institute Grant, Kyungpook National University Hospital (2016).

Compliance with ethical standards

Conflict of Interest The authors declare that they have no conflict of interest.

References

1. Singletary SE, Allred C, Ashley P, Bassett LW, Berry D, Bland KI, Borgen PI, Clark G, Edge SB, Hayes DF, Hughes LL, Hutter RV, Morrow M, Page DL, Recht A, Theriault RL, Thor A, Weaver DL, Wieand HS, Greene FL (2002) Revision of the American joint committee on cancer staging system for breast cancer. J Clin Oncol 20(17):3628–3636
2. Veronesi U, Arnone P, Veronesi P, Galimberti V, Luini A, Rotmensz N, Botteri E, Ivaldi GB, Leonardi MC, Viale G, Sagona A, Paganelli G, Panzeri R, Orecchia R (2008) The value of radiotherapy on metastatic internal mammary nodes in breast cancer. Results on a large series. Ann Oncol 19(9):1553–1560. doi:10.1093/annonc/mdn183
3. Stemmer SM, Rizel S, Hardan I, Adamo A, Neumann A, Goffman J, Brenner HJ, Pfeffer MR (2003) The role of irradiation of the internal mammary lymph nodes in high-risk stage II to IIIA breast cancer patients after high-dose chemotherapy: a prospective sequential nonrandomized study. J Clin Oncol 21(14):2713–2718. doi:10.1200/JCO.2003.09.096
4. Thorsen LB, Offersen BV, Dano H, Berg M, Jensen I, Pedersen AN, Zimmermann SJ, Brodersen HJ, Overgaard M, Overgaard J (2015) DBCG-IMN: a population-based cohort study on the effect of internal mammary node irradiation in early node-positive breast cancer. J Clin Oncol. doi:10.1200/JCO.2015.63.6456
5. Poortmans PM, Collette S, Kirkove C, Van Limbergen E, Budach V, Struikmans H, Collette L, Fourquet A, Maingon P, Valli M, De Winter K, Marnitz S, Barillot I, Scandolaro L, Vonk E, Rodenhuis C, Marsiglia H, Weidner N, van Tienhoven G, Glanzmann C, Kuten A, Arriagada R, Bartelink H, Van den Bogaert W, Oncology ER, Breast Cancer G (2015) Internal mammary and medial supraclavicular irradiation in breast cancer. N Engl J Med 373(4):317–327. doi:10.1056/NEJMoa1415369
6. Chen RC, Lin NU, Golshan M, Harris JR, Bellon JR (2008) Internal mammary nodes in breast cancer: diagnosis and implications for patient management—A systematic review. J Clin Oncol 26(30):4981–4989. doi:10.1200/JCO.2008.17.4862
7. Darby SC, Ewertz M, McGale P, Bennet AM, Blom-Goldman U, Bronnum D, Correa C, Cutter D, Gagliardi G, Gigante B, Jensen MB, Nisbet A, Peto R, Rahimi K, Taylor C, Hall P (2013) Risk of ischemic heart disease in women after radiotherapy for breast cancer. N Engl J Med 368(11):987–998. doi:10.1056/NEJMoa1209825
8. Byrd DR, Dunnwald LK, Mankoff DA, Anderson BO, Moe RE, Yeung RS, Schubert EK, Eary JF (2001) Internal mammary lymph node drainage patterns in patients with breast cancer documented by breast lymphoscintigraphy. Ann Surg Oncol 8(3):234–240
9. Carcoforo P, Sortini D, Feggi L, Feo CV, Soliani G, Panareo S, Corcione S, Querzoli P, Maravegias K, Lanzara S, Liboni A (2006) Clinical and therapeutic importance of sentinel node biopsy of the internal mammary chain in patients with breast cancer: a single-center study with long-term follow-up. Ann Surg Oncol 13(10):1338–1343. doi:10.1245/s10434-006-9062-4
10. Madsen E, Gobardhan P, Bongers V, Albregts M, Burgmans J, De Hooge P, Van Gorp J, van Dalen T (2007) The impact on post-surgical treatment of sentinel lymph node biopsy of internal mammary lymph nodes in patients with breast cancer. Ann Surg Oncol 14(4):1486–1492. doi:10.1245/s10434-006-9230-6
11. Berg WA, Gutierrez L, NessAiver MS, Carter WB, Bhargavan M, Lewis RS, Ioffe OB (2004) Diagnostic accuracy of mammography, clinical examination, US, and MR imaging in preoperative assessment of breast cancer. Radiology 233(3):830–849. doi:10.1148/radiol.2333031484
12. Plana MN, Carreira C, Muriel A, Chiva M, Abraira V, Emparanza JI, Bonfill X, Zamora J (2012) Magnetic resonance imaging in the preoperative assessment of patients with primary breast cancer: systematic review of diagnostic accuracy and meta-analysis. Eur Radiol 22(1):26–38. doi:10.1007/s00330-011-2238-8
13. Cermik TF, Mavi A, Basu S, Alavi A (2008) Impact of FDG PET on the preoperative staging of newly diagnosed breast cancer. Eur J Nucl Med Mol Imaging 35(3):475–483. doi:10.1007/s00259-007-0580-5
14. Groheux D, Espie M, Giacchetti S, Hindie E (2013) Performance of FDG PET/CT in the clinical management of breast cancer. Radiology 266(2):388–405. doi:10.1148/radiol.12110853
15. Aukema TS, Straver ME, Peeters MJ, Russell NS, Gilhuijs KG, Vogel WV, Rutgers EJ, Olmos RA (2010) Detection of extra-axillary lymph node involvement with FDG PET/CT in patients with stage II-III breast cancer. Eur J Cancer 46(18):3205–3210. doi:10.1016/j.ejca.2010.07.034
16. Kinoshita T, Odagiri K, Andoh K, Doiuchi T, Sugimura K, Shiotani S, Asaga T (1999) Evaluation of small internal mammary lymph node metastases in breast cancer by MRI. Radiat Med 17(3):189–193
17. Jochelson MS, Lebron L, Jacobs SS, Zheng J, Moskowitz CS, Powell SN, Sacchini V, Ulaner GA, Morris EA, Dershaw DD (2015) Detection of internal mammary adenopathy in patients with breast cancer by PET/CT and MRI. AJR Am J Roentgenol 205(4):899–904. doi:10.2214/AJR.14.13804
18. An YY, Kim SH, Kang BJ, Lee AW (2015) Comparisons of positron emission tomography/computed tomography and ultrasound imaging for detection of internal mammary lymph node metastases in patients with breast cancer and pathologic correlation by ultrasound-guided biopsy procedures. J Ultrasound Med 34(8):1385–1394. doi:10.7863/ultra.34.8.1385
19. Allred DC, Harvey JM, Berardo M, Clark GM (1998) Prognostic and predictive factors in breast cancer by immunohistochemical analysis. Mod Pathol 11(2):155–168
20. Wolff AC, Hammond ME, Hicks DG, Dowsett M, McShane LM, Allison KH, Allred DC, Bartlett JM, Bilous M, Fitzgibbons P, Hanna W, Jenkins RB, Mangu PB, Paik S, Perez EA, Press MF, Spears PA, Vance GH, Viale G, Hayes DF, American Society of Clinical O, College of American P (2013) Recommendations for human epidermal growth factor receptor 2 testing in breast cancer: american society of clinical oncology/college of American pathologists clinical practice guideline update. J Clin Oncol 31(31):3997–4013. doi:10.1200/JCO.2013.50.9984
21. Caceres E (1963) Incidence of metastasis in the internal mammary chain in operable carcinoma of the breast and 5 year results. Acta Unio Int Contra Cancrum 19:1566–1569
22. Veronesi U, Cascinelli N, Greco M, Bufalino R, Morabito A, Galluzzo D, Conti R, De Lellis R, Delle Donne V, Piotti P et al (1985) Prognosis of breast cancer patients after mastectomy and dissection of internal mammary nodes. Ann Surg 202(6):702–707

23. Sardanelli F, Boetes C, Borisch B, Decker T, Federico M, Gilbert FJ, Helbich T, Heywang-Kobrunner SH, Kaiser WA, Kerin MJ, Mansel RE, Marotti L, Martincich L, Mauriac L, Meijers-Heijboer H, Orecchia R, Panizza P, Ponti A, Purushotham AD, Regitnig P, Del Turco MR, Thibault F, Wilson R (2010) Magnetic resonance imaging of the breast: recommendations from the EUSOMA working group. Eur J Cancer 46(8):1296–1316. doi:10.1016/j.ejca.2010.02.015
24. Sardanelli F (2010) Additional findings at preoperative MRI: a simple golden rule for a complex problem? Breast Cancer Res Treat 124(3):717–721. doi:10.1007/s10549-010-1144-0
25. Orel S (2008) Who should have breast magnetic resonance imaging evaluation? J Clin Oncol 26(5):703–711. doi:10.1200/JCO.2007.14.3594
26. Wang CL, Eissa MJ, Rogers JV, Aravkin AY, Porter BA, Beatty JD (2013) 18F-FDG PET/CT-positive internal mammary lymph nodes: pathologic correlation by ultrasound-guided fine-needle aspiration and assessment of associated risk factors. AJR Am J Roentgenol 200(5):1138–1144. doi:10.2214/AJR.12.8754
27. Huang O, Wang L, Shen K, Lin H, Hu Z, Liu G, Wu J, Lu J, Shao Z, Han Q, Shen Z (2008) Breast cancer subpopulation with high risk of internal mammary lymph nodes metastasis: analysis of 2269 Chinese breast cancer patients treated with extended radical mastectomy. Breast Cancer Res Treat 107(3):379–387. doi:10.1007/s10549-007-9561-4
28. Eubank WB, Mankoff DA, Takasugi J, Vesselle H, Eary JF, Shanley TJ, Gralow JR, Charlop A, Ellis GK, Lindsley KL, Austin-Seymour MM, Funkhouser CP, Livingston RB (2001) 18fluorodeoxyglucose positron emission tomography to detect mediastinal or internal mammary metastases in breast cancer. J Clin Oncol 19(15):3516–3523
29. Mack M, Chetlen A, Liao J (2015) Incidental internal mammary lymph nodes visualized on screening breast MRI. AJR Am J Roentgenol 205(1):209–214. doi:10.2214/AJR.14.13586
30. Ray KM, Munir R, Wisner DJ, Azziz A, Holland BC, Kornak J, Joe BN (2015) Internal mammary lymph nodes as incidental findings at screening breast MRI. Clin Imaging 39(5):791–793. doi:10.1016/j.clinimag.2015.05.011